

Detection of 10-nm Superparamagnetic Iron Oxide Nanoparticles Using Exchange-Biased GMR Sensors in Wheatstone Bridge

L. Li¹, K. Y. Mak¹, C. W. Leung², S. M. Ng², Z. Q. Lei¹, and P. W. T. Pong¹

¹Department of Electrical and Electronic Engineering, The University of Hong Kong, Hong Kong

²Department of Applied Physics, Hong Kong Polytechnic University, Hong Kong

We demonstrated the use of exchange-biased giant magnetoresistance (GMR) sensors in Wheatstone bridge for the detection of 10-nm superparamagnetic iron oxide nanoparticles (SPIONs). The SPIONs were synthesized via coprecipitation method, exhibiting a superparamagnetic behavior with saturation magnetization of 57 emu/g. The output voltage signal of the Wheatstone bridge exhibits log-linear function of the concentration of SPIONs (from 10 ng/ml to 0.1 mg/ml), making the sensors suitable for use as a SPION concentration detector. Thus the combination of 10 nm SPIONs and the exchange-biased GMR sensors has potential to be used in the bio-detection applications where ultra-small bio-labels are needed.

Index Terms—Giant magnetoresistance (GMR), magnetic sensor, superparamagnetic nanoparticles.

I. INTRODUCTION

MAGNETIC biodetection based on magnetic particles has been extensively studied in the past decades. The basic principle is first labeling the targeting biomolecules with magnetic particles, and then these attached magnetic particles are captured by target-probe biomolecular recognition and measured by magnetic sensors. There are remarkable advantages to use magnetic particles in the detection of biomolecules [1]. Their magnetic properties can be very stable, not affected by chemical reaction or photo-bleaching. The magnetic particles can be remotely manipulated by using magnetic field gradients without the interference or screening from the surrounding biomaterials. Previous work in this field has shown that there are two cost-effective techniques for detecting the magnetic particles: superconducting quantum interference device (SQUID) magnetometer and magnetoresistance sensor [2], [3]. In the latter, giant magnetoresistance (GMR) sensor has attracted lots of attentions being inspired by their successful applications in hard disk drives and magnetic recording [4], [5]. Compared to SQUID-based magnetic bio-detection, the GMR technology exhibits the advantages of room-temperature operation, low-power consumption, less complex instruments, compact-in-size and portable, and more flexible implementation [6]. Thus GMR sensor has become a hot choice in magnetic bio-detection.

Bio-detection generally aims at detecting the concentration of specific biological molecules in solution [7]. The magnetic biosensor system utilizing GMR sensor called BARC is firstly demonstrated by a group at the Naval Research Laboratory and NVE Corporation [3], [7]. The superior performance of magnetic bio-detection utilizing GMR multilayer sensor than fluorescent bio-detection was demonstrated by another German

research group [8]. Recently, a lateral flow immunoassay [9], an analytical model for the quantification of protein interaction [10] and a quantitative bio-molecular sensing station [11] based on GMR sensor array were presented by the groups from USA, Spain, and Portugal. However, most commercially available magnetic particles used as bio-probes for bio-detection by these groups tend to be micron or submicron sized. Their larger sizes do not match with the size of typical DNA fragments or protein targets in biological detection. In order to achieve ultra-high sensitivity of bio-detection, the size of magnetic bio-labels with a diameter less than 20 nm are desirable. It is a great challenge to detect such tiny magnetic nanoparticles because their magnetic moments are relatively low due to their limited size [5].

In this paper, we investigated the possibility of detecting superparamagnetic iron oxide nanoparticle (SPIONs) with diameter of 10 nm utilizing GMR sensors in Wheatstone bridge. The superparamagnetism of SPIONs indicates that the particle agglomeration can be avoided when there is no external magnetic field. The ultra-small size of SPIONs can be more comparable to that of the conjugating biomolecules so that they would not block biomolecular interactions [6]. We find that the 10-nm SPIONs can be detected by the exchange-biased GMR sensors in our experimental setup. This may make possible the application of 10-nm SPIONs as bio-labels utilizing the exchange-biased GMR sensors as detectors in magnetic bio-detection.

II. EXPERIMENTS

Superparamagnetic iron oxide nanoparticles (SPIONs) were synthesized based on the chemical coprecipitation of ferrous and ferric salts in alkaline aqueous solution. This is a simple and straightforward method without involving complicated experimental setup, as described in the previous paper [12], [13]. The size and morphology of the SPIONs were characterized by transmission electron microscopy (TEM, Philips CM100). The magnetic property measurement of the SPIONs was carried out at room temperature by using a vibrating sample magnetometer (Lakeshore, VSM 7400).

For the magnetic signal detection, we used bipolar GMR sensor (GF 708) manufacture by Sensitec GmbH in Mainz,

Manuscript received October 31, 2012; revised December 19, 2012; accepted December 31, 2012. Dte of current version June 21, 2013. Corresponding author: P. W. T. Pong (e-mail: ppong@eee.hku.hk).

Color versions of one or more of the figures in this paper are available online at <http://ieeexplore.ieee.org>.

Digital Object Identifier 10.1109/TMAG.2013.2237889

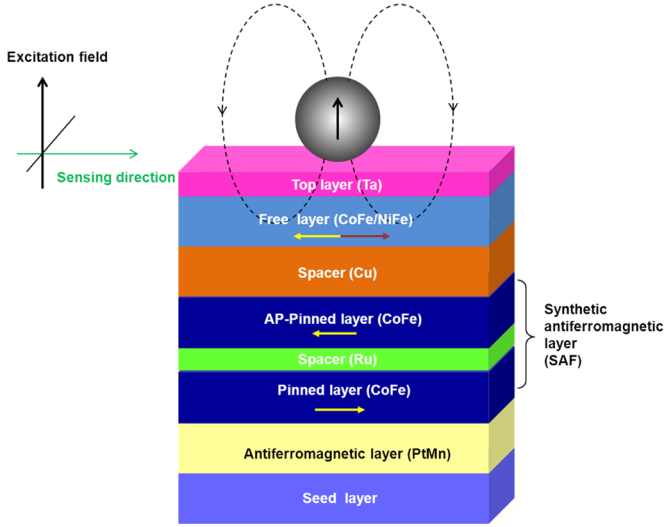


Fig. 1. Schematic structure of the exchange-biased GMR spin valve. It is composed of seed/PtMn/CoFe/Ru/CoFe/Cu/CoFe/NiFe/Ta. The anti-parallel-pinned (AP-pinned) structure provides an alternative pinning mechanism in place of a conventional single antiferromagnet. The arrows indicate the possible magnetization directions. The superparamagnetic iron oxide nanoparticles (SPIONs) are magnetized out-of-plane while the sensors are sensitive to the in-plane component of the stray field emanated from the SPIONs.

Germany. The schematic structure of the spin valve is illustrated in Fig. 1. It consists of a seed layer, antiferromagnetic layer (PtMn), synthetic antiferromagnetic layer, spacer (Cu), free layer (CoFe/NiFe), and top layer (Ta). The synthetic antiferromagnetic layer is composed of two ferromagnetic CoFe layers (pinned layer and antiparallel-pinned layer) sandwiching a Ru layer. The synthetic antiferromagnetic layer is strongly pinned by exchange bias with the underlying antiferromagnetic layer. The exchange-bias effect overcomes the pinned layer stability problem resulting from the pinned layer reversal often observed in conventional spin valves [14]. The SPIONs are magnetized out-of-plane while the sensors are sensitive to the in-plane component of the stray field emanated from the SPIONs.

Each individual sensor consists of four elements in a Wheatstone bridge configuration, as shown in Fig. 2. Two of the elements (R_1 and R_3) serve as the sensing elements, while the other two elements (R_2 and R_4) are shielded as the compensating elements. Every sensing element with a meandering shape consists of four spin valve strips as shown by the arrow in Fig. 2. The dimension of each strip is $1 \mu\text{m} \times 300 \mu\text{m}$. With the on-chip flux concentrators (two trapezoids in Fig. 2), a large sensitivity of 13 mV/V/Oe can be achieved.

The schematic diagram of our measuring setup can be seen in Fig. 3. The GMR sensor was glued to a printed circuit board (PCB) with two part epoxy, and was wire-bonded directly to the pads on the PCB. The Keithley 2400 source meter provides current or voltage for the GMR sensor and the Keithley 2000 digital multimeter is used to measure the Wheatstone bridge output voltage. The Kikusui Bipolar Power Supply PBZ 40-10 was used to supply DC current to the Helmholtz coils to provide an in-plane magnetic field. A perpendicular field was applied by means of a permanent magnet located just below the PCB where the GMR sensor was placed. The perpendicular magnetic

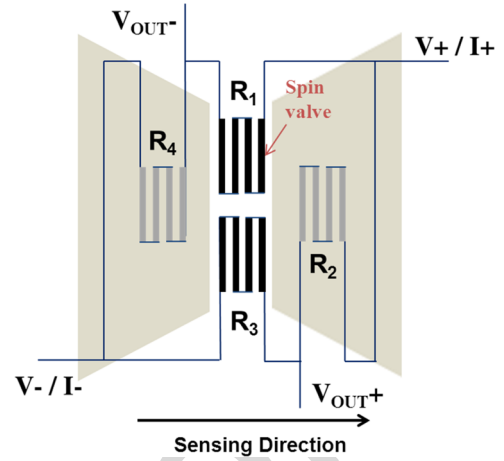


Fig. 2. Layout of a GMR detector: R_1 and R_3 are sensing elements, and R_2 and R_4 are compensating elements of a Wheatstone bridge. The two trapezoids represent two flux concentrators shielding R_2 and R_4 .

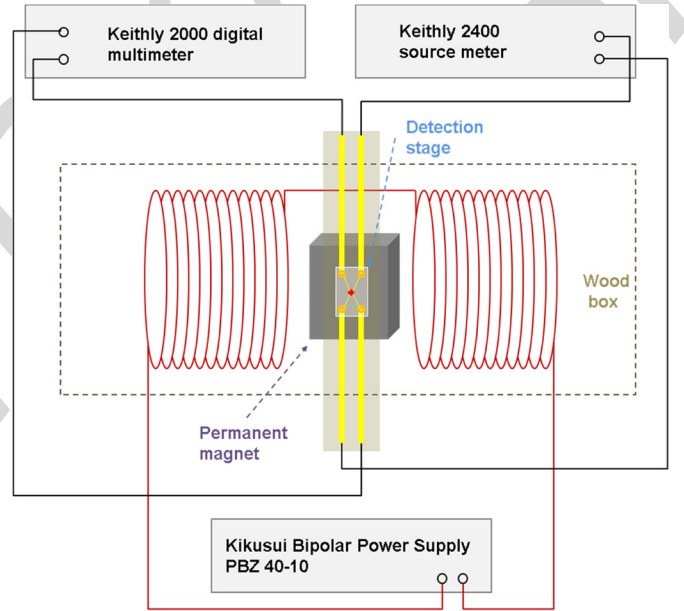


Fig. 3. Schematic diagram of the instrument setup for SPIONs measurement. The Keithly 2400 source meter provides current or voltage for GMR sensor and the Keithly 2000 digital multimeter is used to measure the Wheatstone bridge output voltage. The Kikusui Bipolar Power Supply PBZ 40-10 is used to supply constant DC current to the Helmholtz coils to provide an in-plane magnetic field. A perpendicular field was applied by means of a permanent magnet located just below the PCB where the GMR sensor was placed.

field acting on the particles could be adjusted by modifying the magnet position along the vertical axis.

The SPIONs were dispersed in ethanol by sonication for 5 minutes and vortexed for 15 s. Five different concentrations (10 ng/ml , $0.1 \mu\text{g/ml}$, $1 \mu\text{g/ml}$, $10 \mu\text{g/ml}$, and 0.1 mg/ml) were prepared. The two flux concentrators magnetically shield the two compensating elements (R_2 and R_4 in Fig. 2) in Wheatstone bridge, and thus only the sensing area ($350 \times 10 \mu\text{m}^2$) containing two sensing elements (R_1 and R_3 in Fig. 2) are exposed. After $0.1 \mu\text{L}$ SPION solution in ethanol was drop-casted over the sensing area, the real-time output-voltage of the Wheatstone bridge was recorded every two minutes. The measurement

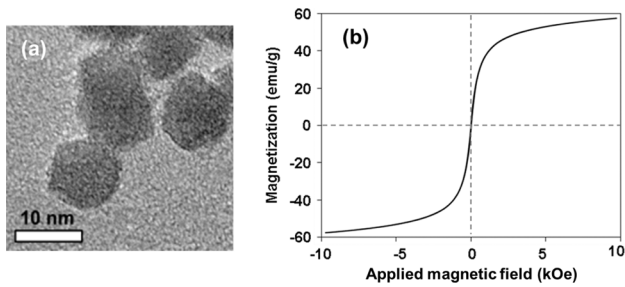


Fig. 4. (a) TEM bright-field image, and (b) VSM result of the superparamagnetic iron oxide nanoparticle (SPIONs) with an average size of 10 nm. The saturation magnetization of the SPIONs is 57 emu/g.

data was conveyed to the PC via GPIB connection for further analysis.

III. RESULTS AND DISCUSSION

The synthesized SPIONs were examined under TEM to evaluate their physical properties. The TEM image of the SPIONs is presented in Fig. 4(a). The SPIONs exhibit a spherical shape with an average size of around 10 nm. The magnetic hysteresis curve of the SPIONs was measured at room temperature by VSM. As shown in Fig. 4(b), the SPIONs display a saturation magnetization of 57 emu/g. The steep initial slope of its magnetization curve and zero magnetic remanence indicate a superparamagnetic behavior with a high magnetic susceptibility. Due to their superparamagnetic characteristic, the SPIONs do not agglomerate after the application of an external magnetic field.

In the measuring setup, a DC current of 2×10^{-5} A was applied to the Wheatstone bridge for output voltage measurements. The transfer curve of the output voltage is shown in Fig. 5. For small resistance change, using constant-current mode is preferred because it offers more linear response and higher sensitivity than using constant-voltage mode [15]. Another reason to use a small DC current is to avoid the sensor heating. The Helmholtz coils were supplied a constant DC current to provide an in-plane magnetic field of 2 Oe, which can place the GMR sensor bridge at its most sensitive operating point as indicated by the red circle in Fig. 5. In order to saturate and polarize the SPIONs, a perpendicular field of 2,000 Oe was applied by the permanent magnet under the sensors. From the magnetization curve in Fig. 4(b), the SPIONs exhibit 45.6 emu/g magnetization with an applied field of 2,000 Oe.

The output voltage signals incurred by the SPIONs in ethanol with five different concentrations (10 ng/ml, 0.1 $\mu\text{g/ml}$, 1 $\mu\text{g/ml}$, 10 $\mu\text{g/ml}$, and 0.1 mg/ml) on the GMR sensors in Wheatstone bridge are plotted in Fig. 6. The signal from the GMR sensors with no treatment serves as the background reference and it was subtracted from the other output signals. The signal from the GMR sensor treated with the same volume of ethanol without SPIONs served as control. After the ethanol evaporated in two minutes, the output voltage of the GMR sensor in Wheatstone bridge exhibited observable increase from its initial value. Treatment with higher SPION concentration led to larger increase while treatment with lower SPION concentration led to smaller increase. The signal drift after two minutes can be ascribed to the slight movement of

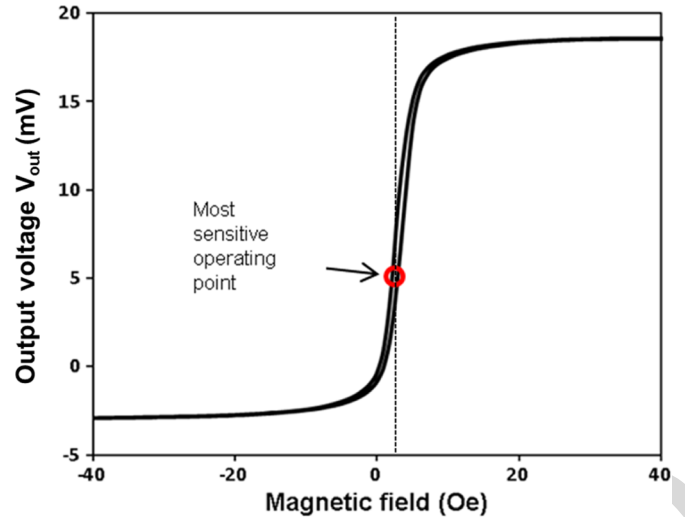


Fig. 5. Transfer curve of the GMR sensor in Wheatstone bridge. The most sensitive operating point is indicated by the red circle.

nanoparticles on the sensor surface which was caused by the slow evaporation of the residual water in ethanol. It can be observed that the ethanol containing no SPIONs produced nearly no changes on the output signal. The output voltage signal (after subtracting the background reference signal) measured over a period of time from 10 min to 60 min was averaged to be the final value of output voltage signal. Here, the final values of the output voltage signals for the five different SPION concentrations are 0.032 mV (10 ng/ml), 0.057 mV (0.1 $\mu\text{g/ml}$), 0.132 mV (1 $\mu\text{g/ml}$), 0.186 mV (10 $\mu\text{g/ml}$), and 0.263 mV (0.1 mg/ml). The relation between the output voltage signal of the GMR sensor and the SPION concentrations is plotted in Fig. 7. The lowest detectable concentration of SPIONs in our setup is 10 ng/ml. The output voltage changes with the logarithm of the SPIONs concentrations from 10 ng/ml to 0.1 mg/ml, and thus the concentration of SPIONs in this range can be deduced from the output signal of the bridge. It was reported that the output signal of a MR sensor exhibits a linear increase with the coverage area of magnetic particles on the sensor surface [8]. In a drop-casted system, the final coverage area of iron oxide nanoparticles on a solid substrate is mainly subject to the “coffee ring” effect [16], and the “ring” size is approximately proportional to the logarithm of the nanoparticle concentration [17]. Since the coverage area of nanoparticles is proportional to the “ring” size, the coverage area is also proportional to the logarithm of the nanoparticle concentration. Therefore, it is sound that the output voltage changes with the logarithm of the SPION concentrations, which is consistent with the results achieved by using a MTJ sensor in a similar drop-casted system [18].

IV. CONCLUSION

We investigated the possibility of using 10-nm SPIONs in a sensing scheme involving exchange-biased GMR sensors. The detection of SPIONs was carried out by drop-casting the SPIONs solution with five different concentrations (10 ng/ml, 0.1 $\mu\text{g/ml}$, 1 $\mu\text{g/ml}$, 10 $\mu\text{g/ml}$, and 0.1 mg/ml) onto the surface of the GMR sensors. The final output voltage of the GMR

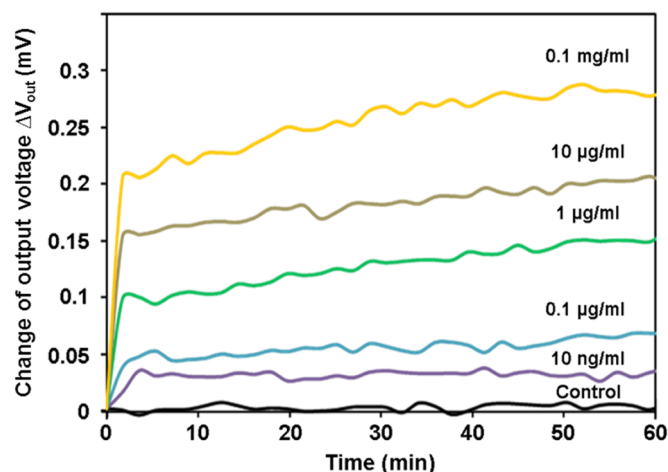


Fig. 6. Output voltage versus time trace for the GMR sensor detection of the SPIONs with five different concentrations from 10 ng/ml to 0.1 mg/ml. Ethanol without SPIONs served as control.

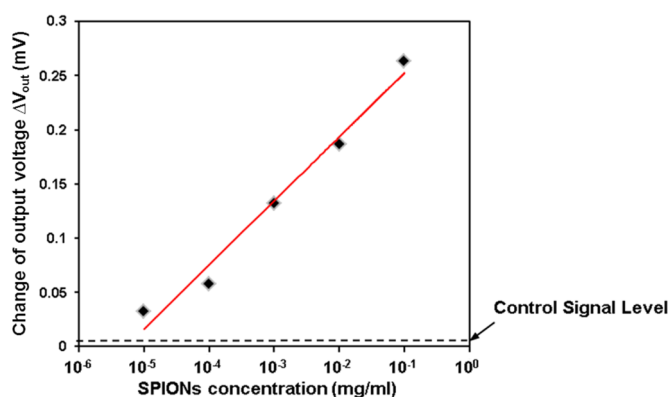


Fig. 7. Plot of the sensor output signal versus the concentration of SPIONs. Ethanol without SPIONs serves as control.

sensor in Wheatstone bridge exhibited a remarkable rising value as the concentration of the detecting SPIONs solution increased. The lowest detectable concentration of SPIONs in our setup is approximately 10 ng/ml. The output voltage changes with the logarithm of the SPIONs concentrations from 10 ng/ml to 0.1 mg/ml, and thus the concentration of SPIONs in this range can be deduced from the output signal of the bridge. This enables the potential application of 10 nm SPIONs as bio-labels with the exchange-biased GMR sensors as detectors in the type of bio-detection where ultra-small bio-labels are needed.

ACKNOWLEDGMENT

This work was supported by the Seed funding Program for Basic Research from the University of Hong Kong, the

RGC-GRF grant (HKU 704911P), and University Grants Council of Hong Kong (Contract No. AoE/P-04/08).

REFERENCES

- [1] J. Rife, M. Miller, P. Sheehan, C. Tamanaha, M. Tondra, and L. Whitman, "Design and performance of GMR sensors for the detection of magnetic microbeads in biosensors," *Sensors Actuators A: Phys.*, vol. 107, pp. 209–218, 2003.
- [2] R. Kotitz, H. Matz, L. Trahms, H. Koch, W. Weitschies, T. Rheinlander, W. Semmler, and T. Bunte, "SQUID based remanence measurements for immunoassays," *IEEE Trans. Appl. Supercond.*, vol. 7, no. 3, pp. 3678–3681, Jun. 1997.
- [3] R. L. Edelstein, C. R. Tamanaha, P. E. Sheehan, M. M. Miller, D. R. Baselt, L. J. Whitman, and R. J. Colton, "The BARC biosensor applied to the detection of biological warfare agents," *Biosensors Bioelectron.*, vol. 14, pp. 805–813, 2000.
- [4] C. Tsang, R. Fontana, T. Lin, D. Heim, B. Gurney, and M. Williams, "Design, fabrication, and performance of spin-valve read heads for magnetic recording applications," *IBM J. Res. Develop.*, vol. 42, pp. 103–116, 1998.
- [5] S. X. Wang and G. Li, "Advances in giant magnetoresistance biosensors with magnetic nanoparticle tags: Review and outlook," *IEEE Trans. Magn.*, vol. 44, no. 7, pp. 1687–1702, Jul. 2008.
- [6] G. Li, S. Sun, R. J. Wilson, R. L. White, N. Pourmand, and S. X. Wang, "Spin valve sensors for ultrasensitive detection of superparamagnetic nanoparticles for biological applications," *Sensors Actuators A: Phys.*, vol. 126, pp. 98–106, 2006.
- [7] D. R. Baselt, G. U. Lee, M. Natesan, S. W. Metzger, P. E. Sheehan, and R. J. Colton, "A biosensor based on magnetoresistance technology," *Biosensors Bioelectron.*, vol. 13, pp. 731–739, 1998.
- [8] J. Schotter, P. B. Kamp, A. Becker, A. Pühler, G. Reiss, and H. Brückl, "Comparison of a prototype magnetoresistive biosensor to standard fluorescent DNA detection," *Biosensors Bioelectron.*, vol. 19, pp. 1149–1156, 2004.
- [9] K. Taton, D. Johnson, P. Guire, E. Lange, and M. Tondra, "Lateral flow immunoassay using magnetoresistive sensors," *J. Magnet. Magn. Mater.*, vol. 321, pp. 1679–1682, 2009.
- [10] R. S. Gaster, L. Xu, S. J. Han, R. J. Wilson, D. A. Hall, S. J. Osterfeld, H. Yu, and S. X. Wang, "Quantification of protein interactions and solution transport using high-density GMR sensor arrays," *Nature Nanotechnol.*, vol. 6, pp. 314–320, 2011.
- [11] D. Serrate, J. M. De Teresa, C. Marquina, J. Marzo, D. Saurel, F. A. Cardoso, S. Cardoso, P. P. Freitas, and M. R. Ibarra, "Quantitative biomolecular sensing station based on magnetoresistive patterned arrays," *Biosensors Bioelectron.*, vol. 35, pp. 206–212, 2012.
- [12] R. Massart, "Preparation of aqueous magnetic liquids in alkaline and acidic media," *IEEE Trans. Magn.*, vol. 17, no. 2, pp. 1247–1248, Mar. 1981.
- [13] L. Li, K. Mak, J. Shi, C. Leung, C. Wong, C. Leung, C. Mak, N. Chan, S. Chan, W. Zhong, C. Shueh, K. Lin, and P. Pong, "Synthesis, characterization, and in vitro biocompatibility assay of Fe₃O₄ nanoparticles," presented at the IUMRS Int. Conf. Asia (IUMRS-ICA), 2011, Paper ID:1359.
- [14] M. Ki-Seok, K. Joo-Chan, R. Jae-Chul, E. Y. Shong, L. Seong Rae, and K. Young Keun, "MR characteristics of synthetic ferrimagnet based spin-valves with different pinning layer thickness ratios," *IEEE Trans. Magn.*, vol. 36, no. 5, pp. 2857–2859, Sep. 2000.
- [15] Mathivanan, PC-based Instrumentation: Concepts and Practice: Prentice-Hall Of India Pvt. Limited, 2007.
- [16] M. Byun, J. Wang, and Z. Lin, "Massively ordered microstructures composed of magnetic nanoparticles," *J. Phys.: Condensed Matter*, vol. 21, p. 264014, 2009.
- [17] X. Shen, C.-M. Ho, and T.-S. Wong, "Minimal size of coffee ring structure," *J. Phys. Chem. B*, vol. 114, pp. 5269–5274, Apr. 29, 2010.
- [18] Z. Lei, C. Leung, L. Li, G. Li, G. Feng, A. Castillo, P. Chen, P. Lai, and P. Pong, "Detection of iron-oxide magnetic nanoparticles using magnetic tunnel junction sensors with conetic alloy," *IEEE Trans. Magn.*, vol. 47, no. 10, pp. 2577–2580, Oct. 2011.

Detection of 10-nm Superparamagnetic Iron Oxide Nanoparticles Using Exchange-Biased GMR Sensors in Wheatstone Bridge

L. Li¹, K. Y. Mak¹, C. W. Leung², S. M. Ng², Z. Q. Lei¹, and P. W. T. Pong¹

¹Department of Electrical and Electronic Engineering, The University of Hong Kong, Hong Kong

²Department of Applied Physics, Hong Kong Polytechnic University, Hong Kong

We demonstrated the use of exchange-biased giant magnetoresistance (GMR) sensors in Wheatstone bridge for the detection of 10-nm superparamagnetic iron oxide nanoparticles (SPIONs). The SPIONs were synthesized via coprecipitation method, exhibiting a superparamagnetic behavior with saturation magnetization of 57 emu/g. The output voltage signal of the Wheatstone bridge exhibits log-linear function of the concentration of SPIONs (from 10 ng/ml to 0.1 mg/ml), making the sensors suitable for use as a SPION concentration detector. Thus the combination of 10 nm SPIONs and the exchange-biased GMR sensors has potential to be used in the bio-detection applications where ultra-small bio-labels are needed.

Index Terms—Giant magnetoresistance (GMR), magnetic sensor, superparamagnetic nanoparticles.

I. INTRODUCTION

MAGNETIC biodetection based on magnetic particles has been extensively studied in the past decades. The basic principle is first labeling the targeting biomolecules with magnetic particles, and then these attached magnetic particles are captured by target-probe biomolecular recognition and measured by magnetic sensors. There are remarkable advantages to use magnetic particles in the detection of biomolecules [1]. Their magnetic properties can be very stable, not affected by chemical reaction or photo-bleaching. The magnetic particles can be remotely manipulated by using magnetic field gradients without the interference or screening from the surrounding biomaterials. Previous work in this field has shown that there are two cost-effective techniques for detecting the magnetic particles: superconducting quantum interference device (SQUID) magnetometer and magnetoresistance sensor [2], [3]. In the latter, giant magnetoresistance (GMR) sensor has attracted lots of attentions being inspired by their successful applications in hard disk drives and magnetic recording [4], [5]. Compared to SQUID-based magnetic bio-detection, the GMR technology exhibits the advantages of room-temperature operation, low-power consumption, less complex instruments, compact-in-size and portable, and more flexible implementation [6]. Thus GMR sensor has become a hot choice in magnetic bio-detection.

Bio-detection generally aims at detecting the concentration of specific biological molecules in solution [7]. The magnetic biosensor system utilizing GMR sensor called BARC is firstly demonstrated by a group at the Naval Research Laboratory and NVE Corporation [3], [7]. The superior performance of magnetic bio-detection utilizing GMR multilayer sensor than fluorescent bio-detection was demonstrated by another German

research group [8]. Recently, a lateral flow immunoassay [9], an analytical model for the quantification of protein interaction [10] and a quantitative bio-molecular sensing station [11] based on GMR sensor array were presented by the groups from USA, Spain, and Portugal. However, most commercially available magnetic particles used as bio-probes for bio-detection by these groups tend to be micron or submicron sized. Their larger sizes do not match with the size of typical DNA fragments or protein targets in biological detection. In order to achieve ultra-high sensitivity of bio-detection, the size of magnetic bio-labels with a diameter less than 20 nm are desirable. It is a great challenge to detect such tiny magnetic nanoparticles because their magnetic moments are relatively low due to their limited size [5].

In this paper, we investigated the possibility of detecting superparamagnetic iron oxide nanoparticle (SPIONs) with diameter of 10 nm utilizing GMR sensors in Wheatstone bridge. The superparamagnetism of SPIONs indicates that the particle agglomeration can be avoided when there is no external magnetic field. The ultra-small size of SPIONs can be more comparable to that of the conjugating biomolecules so that they would not block biomolecular interactions [6]. We find that the 10-nm SPIONs can be detected by the exchange-biased GMR sensors in our experimental setup. This may make possible the application of 10-nm SPIONs as bio-labels utilizing the exchange-biased GMR sensors as detectors in magnetic bio-detection.

II. EXPERIMENTS

Superparamagnetic iron oxide nanoparticles (SPIONs) were synthesized based on the chemical coprecipitation of ferrous and ferric salts in alkaline aqueous solution. This is a simple and straightforward method without involving complicated experimental setup, as described in the previous paper [12], [13]. The size and morphology of the SPIONs were characterized by transmission electron microscopy (TEM, Philips CM100). The magnetic property measurement of the SPIONs was carried out at room temperature by using a vibrating sample magnetometer (Lakeshore, VSM 7400).

For the magnetic signal detection, we used bipolar GMR sensor (GF 708) manufacture by Sensitec GmbH in Mainz,

Manuscript received October 31, 2012; revised December 19, 2012; accepted December 31, 2012. Dte of current version June 21, 2013. Corresponding author: P. W. T. Pong (e-mail: ppong@eee.hku.hk).

Color versions of one or more of the figures in this paper are available online at <http://ieeexplore.ieee.org>.

Digital Object Identifier 10.1109/TMAG.2013.2237889

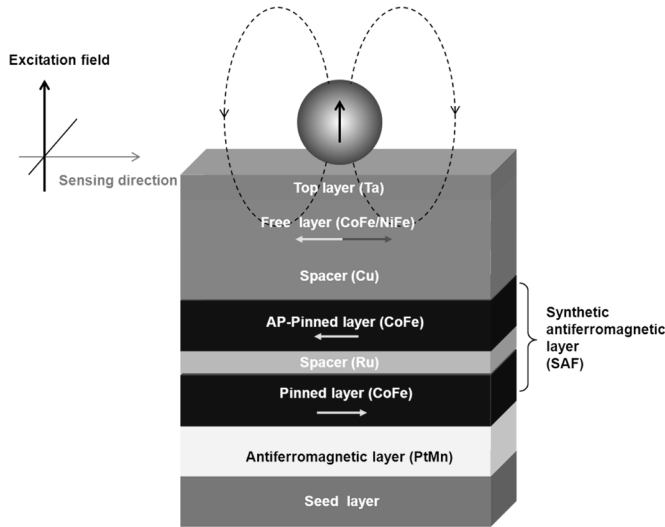


Fig. 1. Schematic structure of the exchange-biased GMR spin valve. It is composed of seed/PtMn/CoFe/Ru/CoFe/Cu/CoFe/NiFe/Ta. The anti-parallel-pinned (AP-pinned) structure provides an alternative pinning mechanism in place of a conventional single antiferromagnet. The arrows indicate the possible magnetization directions. The superparamagnetic iron oxide nanoparticles (SPIONs) are magnetized out-of-plane while the sensors are sensitive to the in-plane component of the stray field emanated from the SPIONs.

Germany. The schematic structure of the spin valve is illustrated in Fig. 1. It consists of a seed layer, antiferromagnetic layer (PtMn), synthetic antiferromagnetic layer, spacer (Cu), free layer (CoFe/NiFe), and top layer (Ta). The synthetic antiferromagnetic layer is composed of two ferromagnetic CoFe layers (pinned layer and antiparallel-pinned layer) sandwiching a Ru layer. The synthetic antiferromagnetic layer is strongly pinned by exchange bias with the underlying antiferromagnetic layer. The exchange-bias effect overcomes the pinned layer stability problem resulting from the pinned layer reversal often observed in conventional spin valves [14]. The SPIONs are magnetized out-of-plane while the sensors are sensitive to the in-plane component of the stray field emanated from the SPIONs.

Each individual sensor consists of four elements in a Wheatstone bridge configuration, as shown in Fig. 2. Two of the elements (R_1 and R_3) serve as the sensing elements, while the other two elements (R_2 and R_4) are shielded as the compensating elements. Every sensing element with a meandering shape consists of four spin valve strips as shown by the arrow in Fig. 2. The dimension of each strip is $1 \mu\text{m} \times 300 \mu\text{m}$. With the on-chip flux concentrators (two trapezoids in Fig. 2), a large sensitivity of 13 mV/V/Oe can be achieved.

The schematic diagram of our measuring setup can be seen in Fig. 3. The GMR sensor was glued to a printed circuit board (PCB) with two part epoxy, and was wire-bonded directly to the pads on the PCB. The Keithley 2400 source meter provides current or voltage for the GMR sensor and the Keithley 2000 digital multimeter is used to measure the Wheatstone bridge output voltage. The Kikusui Bipolar Power Supply PBZ 40-10 was used to supply DC current to the Helmholtz coils to provide an in-plane magnetic field. A perpendicular field was applied by means of a permanent magnet located just below the PCB where the GMR sensor was placed. The perpendicular magnetic

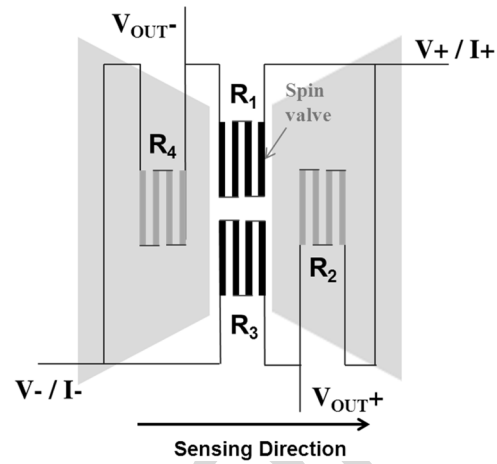


Fig. 2. Layout of a GMR detector: R_1 and R_3 are sensing elements, and R_2 and R_4 are compensating elements of a Wheatstone bridge. The two trapezoids represent two flux concentrators shielding R_2 and R_4 .

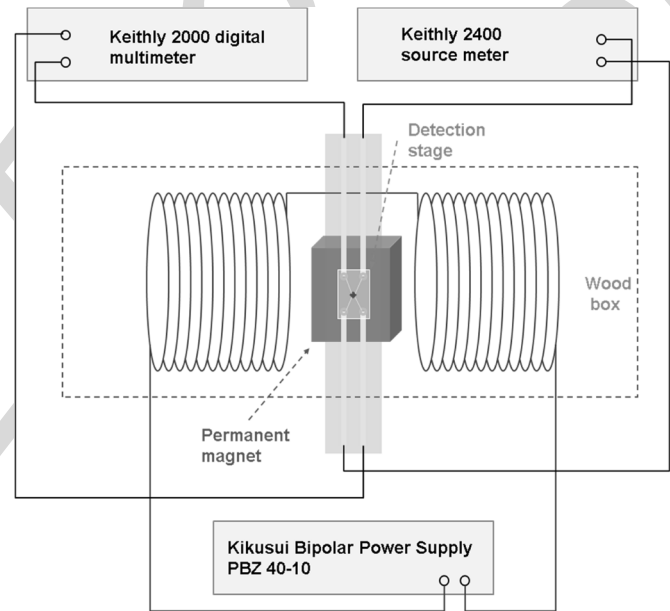


Fig. 3. Schematic diagram of the instrument setup for SPIONs measurement. The Keithley 2400 source meter provides current or voltage for GMR sensor and the Keithley 2000 digital multimeter is used to measure the Wheatstone bridge output voltage. The Kikusui Bipolar Power Supply PBZ 40-10 is used to supply constant DC current to the Helmholtz coils to provide an in-plane magnetic field. A perpendicular field was applied by means of a permanent magnet located just below the PCB where the GMR sensor was placed.

field acting on the particles could be adjusted by modifying the magnet position along the vertical axis.

The SPIONs were dispersed in ethanol by sonication for 5 minutes and vortexed for 15 s. Five different concentrations (10 ng/ml, 0.1 $\mu\text{g}/\text{ml}$, 1 $\mu\text{g}/\text{ml}$, 10 $\mu\text{g}/\text{ml}$, and 0.1 mg/ml) were prepared. The two flux concentrators magnetically shield the two compensating elements (R_2 and R_4 in Fig. 2) in Wheatstone bridge, and thus only the sensing area ($350 \times 10 \mu\text{m}^2$) containing two sensing elements (R_1 and R_3 in Fig. 2) are exposed. After 0.1 μL SPION solution in ethanol was drop-casted over the sensing area, the real-time output-voltage of the Wheatstone bridge was recorded every two minutes. The measurement

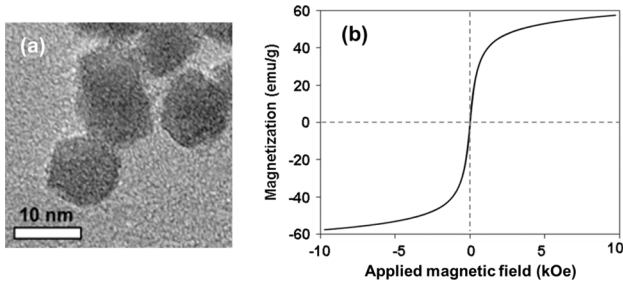


Fig. 4. (a) TEM bright-field image, and (b) VSM result of the superparamagnetic iron oxide nanoparticle (SPIONs) with an average size of 10 nm. The saturation magnetization of the SPIONs is 57 emu/g.

data was conveyed to the PC via GPIB connection for further analysis.

III. RESULTS AND DISCUSSION

The synthesized SPIONs were examined under TEM to evaluate their physical properties. The TEM image of the SPIONs is presented in Fig. 4(a). The SPIONs exhibit a spherical shape with an average size of around 10 nm. The magnetic hysteresis curve of the SPIONs was measured at room temperature by VSM. As shown in Fig. 4(b), the SPIONs display a saturation magnetization of 57 emu/g. The steep initial slope of its magnetization curve and zero magnetic remanence indicate a superparamagnetic behavior with a high magnetic susceptibility. Due to their superparamagnetic characteristic, the SPIONs do not agglomerate after the application of an external magnetic field.

In the measuring setup, a DC current of 2×10^{-5} A was applied to the Wheatstone bridge for output voltage measurements. The transfer curve of the output voltage is shown in Fig. 5. For small resistance change, using constant-current mode is preferred because it offers more linear response and higher sensitivity than using constant-voltage mode [15]. Another reason to use a small DC current is to avoid the sensor heating. The Helmholtz coils were supplied a constant DC current to provide an in-plane magnetic field of 2 Oe, which can place the GMR sensor bridge at its most sensitive operating point as indicated by the red circle in Fig. 5. In order to saturate and polarize the SPIONs, a perpendicular field of 2,000 Oe was applied by the permanent magnet under the sensors. From the magnetization curve in Fig. 4(b), the SPIONs exhibit 45.6 emu/g magnetization with an applied field of 2,000 Oe.

The output voltage signals incurred by the SPIONs in ethanol with five different concentrations (10 ng/ml, 0.1 $\mu\text{g}/\text{ml}$, 1 $\mu\text{g}/\text{ml}$, 10 $\mu\text{g}/\text{ml}$, and 0.1 mg/ml) on the GMR sensors in Wheatstone bridge are plotted in Fig. 6. The signal from the GMR sensors with no treatment serves as the background reference and it was subtracted from the other output signals. The signal from the GMR sensor treated with the same volume of ethanol without SPIONs served as control. After the ethanol evaporated in two minutes, the output voltage of the GMR sensor in Wheatstone bridge exhibited observable increase from its initial value. Treatment with higher SPION concentration led to larger increase while treatment with lower SPION concentration led to smaller increase. The signal drift after two minutes can be ascribed to the slight movement of

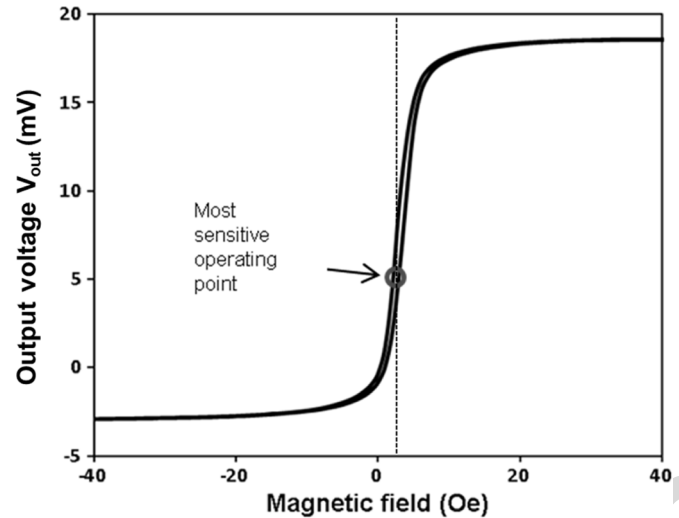


Fig. 5. Transfer curve of the GMR sensor in Wheatstone bridge. The most sensitive operating point is indicated by the red circle.

nanoparticles on the sensor surface which was caused by the slow evaporation of the residual water in ethanol. It can be observed that the ethanol containing no SPIONs produced nearly no changes on the output signal. The output voltage signal (after subtracting the background reference signal) measured over a period of time from 10 min to 60 min was averaged to be the final value of output voltage signal. Here, the final values of the output voltage signals for the five different SPION concentrations are 0.032 mV (10 ng/ml), 0.057 mV (0.1 $\mu\text{g}/\text{ml}$), 0.132 mV (1 $\mu\text{g}/\text{ml}$), 0.186 mV (10 $\mu\text{g}/\text{ml}$), and 0.263 mV (0.1 mg/ml). The relation between the output voltage signal of the GMR sensor and the SPION concentrations is plotted in Fig. 7. The lowest detectable concentration of SPIONs in our setup is 10 ng/ml. The output voltage changes with the logarithm of the SPIONs concentrations from 10 ng/ml to 0.1 mg/ml, and thus the concentration of SPIONs in this range can be deduced from the output signal of the bridge. It was reported that the output signal of a MR sensor exhibits a linear increase with the coverage area of magnetic particles on the sensor surface [8]. In a drop-casted system, the final coverage area of iron oxide nanoparticles on a solid substrate is mainly subject to the “coffee ring” effect [16], and the “ring” size is approximately proportional to the logarithm of the nanoparticle concentration [17]. Since the coverage area of nanoparticles is proportional to the “ring” size, the coverage area is also proportional to the logarithm of the nanoparticle concentration. Therefore, it is found that the output voltage changes with the logarithm of the SPION concentrations, which is consistent with the results achieved by using a MTJ sensor in a similar drop-casted system [18].

IV. CONCLUSION

We investigated the possibility of using 10-nm SPIONs in a sensing scheme involving exchange-biased GMR sensors. The detection of SPIONs was carried out by drop-casting the SPIONs solution with five different concentrations (10 ng/ml, 0.1 $\mu\text{g}/\text{ml}$, 1 $\mu\text{g}/\text{ml}$, 10 $\mu\text{g}/\text{ml}$, and 0.1 mg/ml) onto the surface of the GMR sensors. The final output voltage of the GMR

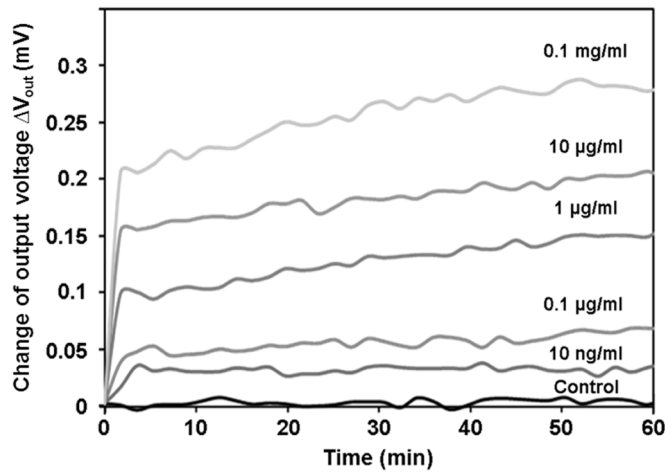


Fig. 6. Output voltage versus time trace for the GMR sensor detection of the SPIONs with five different concentrations from 10 ng/ml to 0.1 mg/ml. Ethanol without SPIONs served as control.

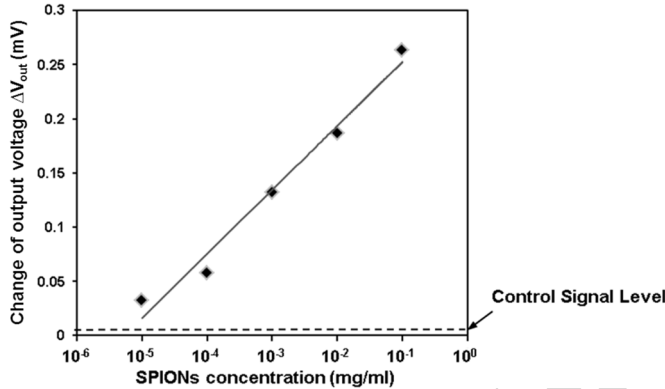


Fig. 7. Plot of the sensor output signal versus the concentration of SPIONs. Ethanol without SPIONs serves as control.

sensor in Wheatstone bridge exhibited a remarkable rising value as the concentration of the detecting SPIONs solution increased. The lowest detectable concentration of SPIONs in our setup is approximately 10 ng/ml. The output voltage changes with the logarithm of the SPIONs concentrations from 10 ng/ml to 0.1 mg/ml, and thus the concentration of SPIONs in this range can be deduced from the output signal of the bridge. This enables the potential application of 10 nm SPIONs as bio-labels with the exchange-biased GMR sensors as detectors in the type of bio-detection where ultra-small bio-labels are needed.

ACKNOWLEDGMENT

This work was supported by the Seed funding Program for Basic Research from the University of Hong Kong, the

RGC-GRF grant (HKU 704911P), and University Grants Council of Hong Kong (Contract No. AoE/P-04/08).

REFERENCES

- [1] J. Rife, M. Miller, P. Sheehan, C. Tamanaha, M. Tondra, and L. Whitman, "Design and performance of GMR sensors for the detection of magnetic microbeads in biosensors," *Sensors Actuators A: Phys.*, vol. 107, pp. 209–218, 2003.
- [2] R. Kotitz, H. Matz, L. Trahms, H. Koch, W. Weitschies, T. Rheinlander, W. Semmler, and T. Bunte, "SQUID based remanence measurements for immunoassays," *IEEE Trans. Appl. Supercond.*, vol. 7, no. 3, pp. 3678–3681, Jun. 1997.
- [3] R. L. Edelstein, C. R. Tamanaha, P. E. Sheehan, M. M. Miller, D. R. Baselt, L. J. Whitman, and R. J. Colton, "The BARC biosensor applied to the detection of biological warfare agents," *Biosensors Bioelectron.*, vol. 14, pp. 805–813, 2000.
- [4] C. Tsang, R. Fontana, T. Lin, D. Heim, B. Gurney, and M. Williams, "Design, fabrication, and performance of spin-valve read heads for magnetic recording applications," *IBM J. Res. Develop.*, vol. 42, pp. 103–116, 1998.
- [5] S. X. Wang and G. Li, "Advances in giant magnetoresistance biosensors with magnetic nanoparticle tags: Review and outlook," *IEEE Trans. Magn.*, vol. 44, no. 7, pp. 1687–1702, Jul. 2008.
- [6] G. Li, S. Sun, R. J. Wilson, R. L. White, N. Pourmand, and S. X. Wang, "Spin valve sensors for ultrasensitive detection of superparamagnetic nanoparticles for biological applications," *Sensors Actuators A: Phys.*, vol. 126, pp. 98–106, 2006.
- [7] D. R. Baselt, G. U. Lee, M. Natesan, S. W. Metzger, P. E. Sheehan, and R. J. Colton, "A biosensor based on magnetoresistance technology," *Biosensors Bioelectron.*, vol. 13, pp. 731–739, 1998.
- [8] J. Schotter, P. B. Kamp, A. Becker, A. Pühler, G. Reiss, and H. Brückl, "Comparison of a prototype magnetoresistive biosensor to standard fluorescent DNA detection," *Biosensors Bioelectron.*, vol. 19, pp. 1149–1156, 2004.
- [9] K. Taton, D. Johnson, P. Guire, E. Lange, and M. Tondra, "Lateral flow immunoassay using magnetoresistive sensors," *J. Magnet. Magn. Mater.*, vol. 321, pp. 1679–1682, 2009.
- [10] R. S. Gaster, L. Xu, S. J. Han, R. J. Wilson, D. A. Hall, S. J. Osterfeld, H. Yu, and S. X. Wang, "Quantification of protein interactions and solution transport using high-density GMR sensor arrays," *Nature Nanotechnol.*, vol. 6, pp. 314–320, 2011.
- [11] D. Serrate, J. M. De Teresa, C. Marquina, J. Marzo, D. Saurel, F. A. Cardoso, S. Cardoso, P. P. Freitas, and M. R. Ibarra, "Quantitative biomolecular sensing station based on magnetoresistive patterned arrays," *Biosensors Bioelectron.*, vol. 35, pp. 206–212, 2012.
- [12] R. Massart, "Preparation of aqueous magnetic liquids in alkaline and acidic media," *IEEE Trans. Magn.*, vol. 17, no. 2, pp. 1247–1248, Mar. 1981.
- [13] L. Li, K. Mak, J. Shi, C. Leung, C. Wong, C. Leung, C. Mak, N. Chan, S. Chan, W. Zhong, C. Shueh, K. Lin, and P. Pong, "Synthesis, characterization, and in vitro biocompatibility assay of Fe₃O₄ nanoparticles," presented at the IUMRS Int. Conf. Asia (IUMRS-ICA), 2011, Paper ID:1359.
- [14] M. Ki-Seok, K. Joo-Chan, R. Jae-Chul, E. Y. Shong, L. Seong Rae, and K. Young Keun, "MR characteristics of synthetic ferrimagnet based spin-valves with different pinning layer thickness ratios," *IEEE Trans. Magn.*, vol. 36, no. 5, pp. 2857–2859, Sep. 2000.
- [15] Mathivanan, PC-based Instrumentation: Concepts and Practice: Prentice-Hall Of India Pvt. Limited, 2007.
- [16] M. Byun, J. Wang, and Z. Lin, "Massively ordered microstructures composed of magnetic nanoparticles," *J. Phys.: Condensed Matter*, vol. 21, p. 264014, 2009.
- [17] X. Shen, C.-M. Ho, and T.-S. Wong, "Minimal size of coffee ring structure," *J. Phys. Chem. B*, vol. 114, pp. 5269–5274, Apr. 29, 2010.
- [18] Z. Lei, C. Leung, L. Li, G. Li, G. Feng, A. Castillo, P. Chen, P. Lai, and P. Pong, "Detection of iron-oxide magnetic nanoparticles using magnetic tunnel junction sensors with conetic alloy," *IEEE Trans. Magn.*, vol. 47, no. 10, pp. 2577–2580, Oct. 2011.